# JAST (Journal of Animal Science and Technology) TITLE PAGE Upload this completed form to website with submission

ARTICLE INFORMATION	Fill in information in each box below	
Article Type	Research article	
Article Title (within 20 words without abbreviations)	Differential Effects of Low- and High-Dose Gamma Irradiation on Hanwoo Muscle-Derived Satellite Cell Morphology and Gene Expression	
Running Title (within 10 words)	Gamma Dose Effects on Hanwoo Satellite Cells	
Author	Sang Hun Park <sup>1,#</sup> , Hyeong Cheol Moon <sup>2,#</sup> , Sol-Hee Lee <sup>1</sup> , Beob Mo Ku <sup>1</sup> , Byung Jun Min <sup>3</sup> , Young Seok Park <sup>2,*</sup> , Jung Seok Choi <sup>1,*</sup>	
Affiliation	1Department of Animal Science, Chungbuk National University, Cheongju 28644, Republic of Korea 2Department of Neurosurgery, Chungbuk National University Hospital, Chungbuk National University College of Medicine, Cheongju, Republic of Korea 3Department of Radiation Oncology, Chungbuk National University Hospital, Chungbuk National University College of Medicine, Cheongju, Republic of Korea	
ORCID (for more information, please visit https://orcid.org)	Sang Hun Park (https://orcid.org/0000-0003-4804-0848) Hyeong Cheol Moon (https://orcid.org/0000-0002-2087-5352) Sol-Hee Lee (https://orcid.org/0000-0003-1124-7095) Beob Mo Ku (https://orcid.org/0009-0009-0814-2007) Byung Jun Min (https://orcid.org/0000-0002-3066-3513) Young Seok Park (https://orcid.org/0000-0001-7685-6292) Jung Seok Choi (https://orcid.org/0000-0001-8033-0410)	
Competing interests	No potential conflict of interest relevant to this article was reported.	
Funding sources State funding sources (grants, funding sources, equipment, and supplies). Include name and number of grant if available.	This work was supported by Chungbuk National University BK21 program (2025)	
Acknowledgements	Not applicable.	
Availability of data and material	Upon reasonable request, the datasets of this study can be available from the corresponding author.	
Authors' contributions Please specify the authors' role using this form.	Conceptualization: Park SH, Moon HC, Park YS, Choi JS Data curation: Park SH, Moon HC, Lee SH, Ku BM, Min BJ Formal analysis: Park SH, Moon HC, Lee SH Methodology: Park SH, Moon HC, Lee SH Software: Park SH, Moon HC Validation: Park SH, Moon HC Investigation: Park SH, Park YS, Choi JS Writing - original draft: Park SH, Moon HC, Lee SH Writing - review & editing: Park SH, Moon HC, Lee SH, Ku BM, Min BJ, Park YS, Choi JS	
Ethics approval and consent to participate	The animal research protocol received approval from the Chungbuk National University Institutional Animal Care and Use Committee.	

## 6 CORRESPONDING AUTHOR CONTACT INFORMATION

For the corresponding author (responsible for correspondence, proofreading, and reprints)	Fill in information in each box below	
First name, middle initial, last name	Jung Seok Choi	
Email address – this is where your proofs will be sent	jchoi@chungbuk.ac.kr	
Secondary Email address		
Address	Department of Animal Science, Chungbuk National University, Cheongju 28644, Republic of Korea	
Cell phone number	+82-10-3235-2127	
Office phone number	+82-43-261-2551	
Fax number	+82-43-273-2240	

For the corresponding author (responsible for correspondence, proofreading, and reprints)	Fill in information in each box below	
First name, middle initial, last name	Young Seok Park	
Email address – this is where your proofs will be sent	youngseokparkmd@gmail.com	
Secondary Email address		
Address	Department of Neurosurgery, Chungbuk National University Hospital, Chungbuk National University College of Medicine, Cheongju, Republic of Korea	
Cell phone number	+82-10-5418-8453	
Office phone number	+82-43-269-6080	
Fax number	+82-43-273-1614	

#### **Abstract**

10

11

12

13

14

15

16

17

18

19

20

21

22

2324

25

26

27

28

29

30

31

3233

34

Gamma irradiation is extensively employed for sterilization purposes in both the medical and food sectors. Recently, its use in cultured meat technology has emerged as an area of interest. Despite this, the specific impacts of gamma radiation on muscle stem cells that are crucial for cultured meat biomanufacture have not been well delineated, especially in livestock like Hanwoo. This study investigated the dose-dependent influence of targeted gamma irradiation on the morphology, viability, and gene expression profile of Hanwoo muscle-derived satellite cells utilizing a clinically certified Gamma Knife platform. Satellite cells were isolated from Hanwoo skeletal muscle by fluorescence-activated cell sorting (FACS) and exposed to gamma irradiation at Con(0), 2, 10, and 20 Gy. Following irradiation, cells were maintained under conditions promoting proliferation or differentiation. We evaluated cellular viability, morphological characteristics, and transcriptional levels of myogenic (MYF5, MYOD1, MYOG, MYH2) and cell cycle regulatory (TP21, TP53) genes. Exposure to high-dose gamma radiation (10 and 20 Gy) markedly reduced satellite cell proliferation, viability, and substrate attachment, also resulting in increased cell size and elevated expression of senescence-related markers TP21 and TP53 (p < 0.05). A dose-dependent downregulation of myogenic gene expression was recorded, notably for MYF5, MYOD1, and MYOG. Importantly, low-dose irradiation (2 Gy) led to a transient elevation in MYH2 expression while preserving cell viability and structural integrity, indicating possible hormetic responses (p < 0.05). Overall, gamma irradiation affects Hanwoo satellite cells in a dose-dependent manner, with higher doses promoting cellular aging and loss of myogenic potential, while lower doses may stimulate defense or differentiation-associated mechanisms. These results highlight the critical need for careful dose optimization when utilizing irradiation in cultured meat processes. Additional research is needed to delineate non-lethal radiation limits and confirm observations in vivo.

Keywords (3 to 6): Hanwoo satellite cells, Gamma radiation, Cell hypertrophy, Radiation dose-response

# Introduction

35

36

37

38

39

40

41

42

43

44

45

46

47

48

49

50

51

52

53

54

55

56

57

58

59

60

61

62

63

64

65

66

67

68

69

Ionizing radiation (IR) denotes electromagnetic waves or particle beams possessing enough energy to ionize atoms or molecules, which results in various physicochemical and biological changes. IR is recognized for causing significant biological harm, including DNA double-strand breaks, chromosomal aberrations, apoptosis, necrosis, and cellular senescence [1]. Historically, IR has been widely applied in oncology to specifically target rapidly proliferating tumor cells, where exposure to high-dose irradiation induces cell cycle arrest and leads to irreversible cellular demise [2]. However, in cultured meat production systems, it is essential to implement irradiation protocols that minimize potential damage to host cells while maintaining process efficiency and cellular functionality. Cultured meat comprises cell-based products generated through the *in vitro* expansion and differentiation of animal stem cells. Skeletal muscle satellite cells represent the primary stem cell type utilized for cultured meat development. These cells are located between the basal lamina and sarcolemma of muscle fibers and typically exist in a quiescent state. Upon activation by injury or stress signals, they proliferate and differentiate to facilitate muscle repair and regeneration [3]. Irradiation at doses lower than those typically used in oncology may not only serve as an effective approach to secure microbial safety in the culture medium but also provide an opportunity to explore potential hormesis-like responses in muscle-derived cells [4]. Expanding on this concept, understanding the effects of radiation on muscle-derived cells under scalable production conditions could offer valuable insights for large-scale cultured meat manufacturing. Such understanding would allow for the development of irradiation-based strategies to mitigate contamination risks in culture media or biomaterials. To meet this objective, a stereotactic radiosurgery (SRS) system capable of precise gamma radiation delivery at the submillimeter scale was employed. This technology, originally designed for treatments such as brain tumor therapy, provides high targeting fidelity and reproducibility, rendering it advantageous for in vitro irradiation of delicate cell types. The incorporation of cone-beam computed tomography (CBCT) into the system enables accurate localization and targeting of the irradiation zone. In the food industry, gamma radiation sourced from cobalt-60 is widely utilized as a non-thermal sterilization method [5]. Cultured meat offers several advantages, including improved food safety, enhanced environmental sustainability, and better animal welfare. Despite its promise, achieving large-scale production remains challenging, especially with respect to ensuring microbiological safety while maintaining the cellular viability and regenerative functions. Low-dose electron beam irradiation has been shown to sterilize fetal bovine serum (FBS), and the efficacy of gamma irradiation for sterilizing various biomaterials has also been confirmed [6, 7]. In C2C12 myoblasts, exposure to 10–20 Gy has been reported to induce apoptosis and delay myotube formation, whereas doses below 6 Gy substantially reduced these effects [8]. Therefore, SRS-based gamma irradiation may, at low doses, induce mild hormesis-like effects in muscle-derived stem cells, thereby promoting cellular adaptation and preserving functionality during the cultured meat production process [8]. The majority of prior investigations assessing radiation impacts on

muscle have utilized whole-body gamma or X-ray exposure models in rodents, such as mice and rats [9], or have concentrated on human-sourced satellite cells [10]. Although a number of investigations have examined muscle regeneration and satellite cell responses to radiation in livestock species, such as pigs and cattle, relevant studies are few. Moreover, spatially targeted irradiation of muscle-derived stem cells originating from livestock has not been extensively investigated. Elucidating the responses of Hanwoo muscle stem cells to radiation-induced stress is crucial for both the advancement of veterinary and livestock biotechnology and the development of safe, high-quality cultured meat from valuable breeds.

In this study, we implemented a standardized *in vitro* gamma irradiation protocol to evaluate the impact of high-dose radiation on the morphology, viability, and gene expression of Hanwoo satellite cells. We assessed cell size and viability, and measured the expression of critical genes associated with muscle differentiation and cell cycle regulation using quantitative real-time PCR. The molecular analyses provided the ability to identify early cellular responses that could not be detected through morphological analysis alone. By combining morphological assessments with gene expression data, this study advances knowledge regarding gamma radiation effects on the functional characteristics of bovine satellite cells and offers implications for optimizing quality control in cultured meat production.

## **Materials and Methods**

#### Hanwoo muscle-derived cell isolation and fluorescence-activated cell sorting (FACS)

Top round muscle tissues were obtained from a 25-month-old female Hanwoo at Donga Food Co., Ltd. The samples were transported to the laboratory in an icebox. In Korea, there is currently no commercial source or tissue bank for bovine primary cells. Because research access to commercial slaughterhouses is limited, it was not possible to collect samples from multiple donor animals at the same time. Therefore, all experiments were performed using cells from one Hanwoo donor, with at least three technical replicates for each treatment to ensure experimental consistency [11]. After delivery, tissues were enzymatically dissociated with collagenase type II solution (Worthington, Cat #LS004176). Connective tissue and muscle satellite cells were then separated by centrifugation at 800 × g for 5 min after digestion. Before FACS, cells were cultured in flasks coated with 6 mg/mL bovine collagen type I (Sigma-Aldrich, Cat #C2124) until they reached confluency. The cells were harvested and suspended in FACS buffer (PBS with 1% bovine serum albumin) for antibody labeling. The antibodies used included APC anti-human CD29 (1:10, BioLegend, Cat #303008), PE-Cy7 anti-human CD56 (1:10, BD Biosciences, Cat #335826), FITC antisheep CD31 (1:10, Bio-Rad, Cat #MCA1097F), and FITC anti-sheep CD45 (1:10,s Bio-Rad, Cat #MCA2220F). Labeling was done at 4°C for 30 min in the dark. Following labeling, cells were rinsed twice with cold PBS and resuspended in growth medium (GM) consisting of Ham's F-10 nutrient mix (Gibco, Cat #11550043) with 20% FBS (BS, Gibco, Cat #16000044) and 1% PSA (penicillin, streptomycin, amphotericin B; Lonza, Cat #17745E). Fluorescence-activated cell sorting was carried out using a FACSAriaTM II Cell Sorter (BD Biosciences) to collect the CD31-/CD45-/CD29+/CD56+ satellite cell fraction [12].

#### Co-60 Gamma Irradiation Using the Gamma Knife System

To achieve precise and reproducible *in vitro* irradiation, the Leksell GammaPlanTM treatment planning software (version 11.3.2, Elekta AB, Stockholm, Sweden) was employed. Suspension-cultured satellite cells were enclosed in a 1.5 mL microtube (MCT-150-C, Axygen, Union City, CA, USA) sealed with Parafilm, and positioned within a tissue-equivalent phantom constructed from polymethyl methacrylate (PMMA), which was designed to replicate cranial geometry and facilitate uniform dose distribution. The location of each tube was verified and aligned through the integrated CBCT system of the Gamma Knife IconTM, enabling accurate co-registration of acquired CBCT images with the planning software. Using these CBCT images, the coordinates for each tube were established, and the irradiation field was defined with a 4 mm collimator based on the 50% isodose line for dose planning. Single-fraction target doses of 2, 10, and 20 Gy were applied to the geometric center of each tube. The 2, 10, and 20 Gy doses were delivered for 3.37, 17.01, and 33.81 minutes, respectively. Control group tubes (0 Gy) were positioned similarly within the Gamma Knife system but were not exposed to Co-60 radiation. Although focused irradiation is characteristic of the Gamma Knife, minimal scatter to adjacent regions may still occur. It should be noted that γ-irradiation in this study was applied exclusively to muscle-derived satellite cells to investigate radiation-induced cellular responses, not for sterilization purposes.

#### Post-irradiation culture

After fluorescence-activated cell sorting (FACS), Hanwoo satellite cells were subjected to  $\gamma$ -irradiation and subsequently maintained under either proliferation or differentiation protocols. For proliferation assays, cells were seeded at a density of 1,800 viable cells/cm² onto flasks coated with 0.05% bovine collagen type I (Sigma-Aldrich, Cat #C2124) and cultured in growth medium (GM). Cultures were maintained for six days under standard incubation taking place at 37 °C in a humidified atmosphere with 5% CO<sub>2</sub>). For differentiation experiments, to minimize potential differences in confluency among treatment groups caused by radiation-induced variation in proliferation rates, a higher seeding density (5,000 viable cells/cm²) was used. Cells were plated on Matrigel-coated flasks (Corning) and maintained in differentiation medium formulated as Dulbecco's Modified Eagle Medium (DMEM, Gibco, Cat #11995065) supplemented with 2% FBS and 1% PSA [11]. This approach ensured that all groups reached comparable confluency levels at the initiation of differentiation, thereby reducing confounding effects associated with unequal growth rates after irradiation. Figure 1 provides a schematic overview of the experimental workflow, illustrating the core design and methodological steps.

#### 140 Total cell, live cell, and viability measurement

- 141 After irradiation, analyses were conducted at three time points: immediately following irradiation (0 day),
- after 1 day in culture, and after 6 days in culture. Cells were harvested using 0.05% trypsin-EDTA (Gibco).
- The numbers of total and live cells, along with viability (%), were determined by an automated cell counter
- (Countess<sup>TM</sup>, Invitrogen) using trypan blue staining.

145146

#### Measurement of cell length, width, and histogram analysis of cell area

- 147 Cell morphology was assessed at 2, 4, and 6 days post-irradiation. Adherent cells were visualized using a
- phase-contrast microscope (EVOS<sup>TM</sup> M5000, Thermo Fisher Scientific). Representative images were
- 149 collected at each time interval. Cell length and width were quantified using ImageJ software (NIH, USA).
- 150 In total, measurements were performed on 270 cells across all experimental groups. Cell area was
- determined by multiplying length and width. The criterion for cell enlargement was established as the mean
- 152 control group area plus two standard deviations (mean + 2SD). Distributions of cell area were visualized as
- histograms generated with matplotlib (Python) [13-15].

154155

#### Reverse transcription quantitative polymerase chain reaction (RT-qPCR)

- Gene expression analysis was performed by harvesting cultured cells, followed by total RNA extraction
- using a Total RNA Extraction Kit (iNtRON Biotechnology, Seongnam-si, Republic of Korea, Cat # 17221),
- according to the manufacturer's instructions. The synthesis of complementary DNA (cDNA) was conducted
- with the High-Capacity cDNA Reverse Transcription Kit (Thermo Fisher, Cat # 4368814). RT-qPCR was
- 160 carried out using Fast qPCR 2 × SYBR Green Master Mix (Cat # EBT-1821). Amplification conditions
- 161 consisted of an initial step at 50 °C for 2 min and 95 °C for 10 min, followed by 40 cycles of 95 °C for 15
- s and annealing at 56 °C for 1 min. The analysis included the genes MYF5, MYOD1, TP21, TP53, MYOG,
- 163 MYH2 and GAPDH. Primer sequences are provided in Table 1. Relative gene expression was determined
- by the  $2^{-\Delta\Delta CT}$  method [16].

165166

#### Statistical analysis

- All experimental data were obtained from a minimum of three independent experiments and are expressed
- as mean ± standard deviation. Statistical analyses were conducted using GraphPad Prism version 10
- 169 (GraphPad Software, San Diego, CA, USA). Comparisons among groups were performed using one-way
- analysis of variance (ANOVA) followed by Tukey's multiple comparison test. A p-value < 0.05 was
- 171 considered statistically significant.

172

173

174

### **Results and discussion**

Dose-dependent effect of radiation on the proliferative capacity of muscle-derived cells

Muscle-derived cells isolated from Hanwoo cattle were suspended in microtubes and subjected to  $\gamma$ radiation at doses of 0, 2, 10, and 20 Gy. Following irradiation, the control group (0 Gy) exhibited the lowest total and live cell counts (p < 0.05). Nevertheless, cell viability, defined as the percentage of live cells among total cells, did not significantly differ between treatment groups (Figure 2A). This observation likely reflects variability introduced during the cell transfer procedure, rather than being a consequence of direct cytotoxicity from irradiation. Trypan blue exclusion analysis demonstrated that  $\gamma$ -irradiation did not affect membrane integrity, indicating that acute  $\gamma$ -radiation exposure does not lead to immediate disruption of the plasma membrane in bovine muscle-derived cells. Following irradiation, the cell suspensions were reseeded at a density of 1,800 cells/cm<sup>2</sup> and cultured for 24 hours. After this incubation period, both total and live cell numbers were markedly higher in the control group than in the irradiated groups (p < 0.05, Figure 2B). This difference likely resulted from reduced cell adhesion efficiency rather than altered proliferation rates. The lower cell counts in the irradiated groups probably result from reduced initial attachment, causing increased cell detachment during early culture. Moreover, in the 10 and 20 Gy groups, cell viability decreased in a dose-dependent manner, suggesting that higher doses of γ-radiation negatively impacted both the ability of cells to attach and survive. By the sixth day of culture, the inhibitory impact of γ-radiation on cell proliferation became more pronounced. Both total and live cell counts remained highest in the control group and were significantly lower in the 10 and 20 Gy groups (p < 0.05, Figure 2C). There was also a parallel dose-dependent reduction in cell viability, providing further evidence of the detrimental effects of  $\gamma$ -radiation on the proliferative capacity of bovine muscle-derived cells (p < 0.05). Gene expression analysis indicated that MYF5 mRNA abundance peaked in the control group but was significantly lower in all irradiated groups (p < 0.05, Figure 2D). Similarly, MYOD1 mRNA, a principal marker for myogenic differentiation, showed a marked dose-dependent decline in the 2 Gy, 10 Gy, and 20 Gy groups (p < 0.05, Figure 2D). Conversely, transcript levels of TP21 (CDKN1A) and TP53 mRNA, both integral to the DNA damage response and regulation of cell cycle arrest, were significantly upregulated in the 20 Gy group (p < 0.05, Figure 2D). These data indicate that high-dose  $\gamma$ -irradiation causes DNA doublestrand breaks and activates G1/S checkpoint signaling, resulting in cell cycle arrest. y-irradiation in suspension did not seem to directly compromise cell membrane integrity, as indicated by the preservation of cell viability immediately after irradiation (Figure 2A). In this investigation, we selected irradiation doses of 2 Gy, 10 Gy, and 20 Gy to represent low, intermediate, and high levels of radiationinduced stress, respectively. These dose selections were based on established biological thresholds frequently referenced in radiobiological and oncological literature. The 2 Gy dose, often considered sublethal, serves as a standard fraction in clinical radiotherapy protocols. The 10 Gy dose causes notable but not fatal DNA damage and is commonly utilized in the management of benign tumors. The 20 Gy dose approximates the lower threshold for inducing severe DNA double-strand breaks and irreversible cell cycle arrest, particularly observed in malignant tumor models. Despite the maintained viability, a decline in cell

175

176

177

178

179

180

181

182

183

184

185

186

187

188

189

190

191

192

193

194

195

196

197

198

199

200

201

202

203

204

205

206

207

208

adhesion after irradiation suggests possible disruptions in the composition or functionality of membrane proteins associated with adhesion. The oxidative stress and genotoxic effects elicited by  $\gamma$ -irradiation may inhibit the ITGB1-FAK signaling axis, and this could decrease adhesion strength and promote cell detachment. Additionally, radiation-mediated suppression or breakdown of cadherins may destabilize adherens junctions, consequently weakening both cell-cell and cell-substrate attachments. Furthermore, cytoskeletal reorganization following irradiation might further undermine the adhesive and migratory properties of cells [17]. Collectively, these molecular and structural disruptions may persist throughout prolonged culture, ultimately limiting the sustained growth and propagation of bovine muscle-derived cells (Figure 2C). The observed upregulation of TP21 and TP53 provides strong evidence for the activation of cell cycle arrest in response to DNA damage. As a source of high-energy photons, γ-irradiation has been widely recognized to generate direct DNA double-strand breaks and initiate the production of reactive oxygen species, leading to a combined effect on membrane protein stability and adhesion signaling [10, 18]. Notably, in contrast to  $\gamma$ -rays, X-rays have been reported to transiently promote adhesion in cancer cells through activation of FAK and integrin signaling mechanisms [19]. Multiple reports indicate that Xray exposure can enhance the expression of adhesion-associated proteins and induce cytoskeletal changes [20, 21]. Consequently, it would be valuable to explore whether low-dose  $\gamma$ -irradiation (<2 Gy) could provoke similar pro-adhesive responses in bovine muscle cells analogous to those seen with X-rays. The Hanwoo population is managed under nationally coordinated breeding and genetic evaluation programs involving performance/progeny testing and routine nationwide dissemination of proven-bull (KPN) semen via artificial insemination, overseen by governmental research and improvement agencies [22]. These longstanding programs have standardized selection pressure at the national scale and shaped breed genetics over

232233

234

235

236

237

238

239

240

241

242

243

244

210

211

212

213

214

215

216

217

218

219

220

221

222

223

224

225

226

227

228

229

230

231

#### **Dose-dependent effect of radiation on cell size**

To assess the impact of  $\gamma$ -irradiation on cell morphology, bovine muscle-derived cells were cultured after exposure and phase-contrast images were captured at specific time points (Figure 3A). Cells in all irradiated groups adhered to the culture plates, and the number of attached cells increased as the culture period progressed. On day 6, distinctly abnormal cell morphologies, such as notably enlarged and flattened cells, were mainly observed in the 20 Gy group. Quantitative analysis of morphological alterations was performed by measuring cell length and width across all groups and time points (Figure 3B). Both length and width increased in correlation with higher radiation doses. Importantly, as the culture duration increased, the disparity in cell sizes between groups became increasingly evident. To further examine the occurrence of unusually enlarged cells, a threshold for enlargement was established using the product of length and width in the control group at each time point. Specifically, this threshold was defined as the mean plus two

the past four decades, which provides contextual support for reproducibility of cellular phenotypes within

this breed framework, even when a single donor is used in a proof-of-concept setting [23].

standard deviations (mean + 2SD) of the area (length × width) in the control group on days 2, 4, and 6. This approach statistically represents roughly the upper 2.5% of a normal distribution, effectively identifying morphological outliers. The calculated thresholds were 9,447.4, 9,689.1, and 12,898.8 µm² for days 2, 4, and 6, respectively, highlighting a gradual increase in cell size within the control group over time. The percentage of cells surpassing these thresholds was determined. On day 2, the frequencies of enlarged cells were 5.19% (Con), 6.30% (2 Gy), 30.74% (10 Gy), and 22.22% (20 Gy). By day 4, the proportions rose to 2.96% (Con), 16.67% (2 Gy), 51.11% (10 Gy), and 65.19% (20 Gy). On day 6, these incidences were 3.33%, 4.07%, 32.59%, and 82.22%, respectively (Figure 3C). The 20 Gy group on day 6 exhibited the most substantial increase in cell enlargement.

Cell enlargement is frequently linked with cellular senescence during prolonged culture [13]. Our results align with previous literature demonstrating that radiation induces senescence in bovine muscle-derived cells [11]. The observed enlargement is most likely attributable to DNA damage caused by radiation, which is corroborated by the upregulation of *TP21* and *TP53* mRNA (Figure 2C). Additionally, radiation has been shown to disrupt the organization of cytoskeletal elements. Several studies report that X-irradiation leads to greater cell spreading, induces cytoskeletal remodeling, and results in increased nuclear size [24]. Early apoptotic processes are closely associated with changes in cytoskeletal proteins, particularly those involving actin filaments and microtubules. Ionizing radiation has been shown to disturb actin filament assembly, cause DNA double-strand breaks, and heighten the production of reactive oxygen species (ROS) [10]. These molecular changes correspond to the morphological features illustrated in Figure 3A and might contribute to the observed reduction in proliferative ability in Figure 2. However, the reversibility of certain morphological changes depends on the radiation dose received. Some investigations have found that cells exposed to sublethal irradiation can regain their typical morphology, suggesting that morphological adaptations to radiation stress may, under specific conditions, be reversible [25].

#### Differential dose effects of irradiation on myogenic differentiation

To determine the impact of  $\gamma$ -irradiation on muscle cell differentiation, bovine muscle-derived cells were irradiated and subsequently cultured in differentiation medium, with phase-contrast microscopy used for assessment at set intervals (Figure 4A). Myotube structures were identified in every experimental group, regardless of irradiation status. For quantitative analysis of myogenic differentiation, relative mRNA expression of key myogenic markers was measured (Figure 4B). The control group displayed the highest MYOG mRNA expression, which was significantly decreased in both the 10 and 20 Gy irradiation groups, signifying a dose-dependent inhibition of late-stage myogenic differentiation (p < 0.05). Notably, MYH2 mRNA expression peaked following 2 Gy exposure, but was markedly suppressed in the 20 Gy group (p < 0.05).

This study demonstrates that gamma irradiation influences bovine muscle-derived satellite cells in a dosedependent manner. Exposure to high doses, such as 10 Gy or 20 Gy, led to marked alterations in cell morphology and a significant reduction in the expression of key myogenic genes, including MYF5, MYOD1, MYOG, and MYH2 mRNA. These results indicate that intense radiation disrupts the normal process of muscle differentiation and induces cell cycle arrest resembling premature senescence. In contrast, low-dose irradiation at 2 Gy elicited a distinct response. In this group, MYH2 mRNA expression was transiently upregulated, with no significant change detected in cell size or viability. This suggests that low levels of radiation may initiate protective or differentiation-associated pathways without inducing persistent cellular damage. Although the present findings reflect transcriptional and morphological alterations rather than permanent genomic changes, the concurrent upregulation of TP21 and TP53 observed in irradiated groups supports the activation of a transient DNA damage response (DDR) and cell cycle checkpoint control. These mechanisms are typically reversible and serve to preserve genomic stability under stress conditions. The mild upregulation of MYH2 at 2 Gy may therefore represent an adaptive, hormetic-like response, in which low-dose irradiation triggers protective signaling and compensatory repair activity rather than mutagenic effects. Potential mechanisms may involve mild mitochondrial activation, attenuation of oxidative stress, or transient enhancement of cellular repair pathways. Further investigation is warranted to elucidate the specific molecular mechanisms involved [17]. Satellite cells play a pivotal role in muscle regeneration and must maintain a balance between proliferation and differentiation in response to physiological cues. The present findings suggest that satellite cells possess the ability to sense the magnitude of radiation exposure and adjust their responses accordingly. High radiation doses seem to suppress their normal functionality, whereas low doses may transiently facilitate differentiation processes [26]. The irradiation protocol employed in this study warrants consideration. While the Gamma Knife system offers precise targeting capabilities, it generates a steep dose gradient from the center to the periphery, potentially resulting in heterogeneous radiation exposure among cells within the same treatment cohort. Given the radiosensitivity of satellite cells, even subtle dose variations could contribute to differing cellular outcomes. Upcoming experiments should incorporate detailed dose mapping approaches, such as Monte Carlo simulations or single-cell level analysis, to better elucidate cellular responses to minute fluctuations in radiation. If these observations are mirrored in vivo, satellite cells compromised by radiation could lose their regenerative capacity and possibly secrete detrimental factors affecting adjacent cells, thereby exacerbating muscle injury post-radiotherapy. Thus, defining the threshold dose that differentiates reversible from irreversible cellular effects is critical. Future research should prioritize investigations into the cellular consequences of low-dose gamma irradiation. Investigating these lower doses could facilitate the identification of advantageous cellular responses that support muscle regeneration while minimizing the risk of long-term adverse effects.

279

280

281

282

283

284

285

286

287

288

289

290

291

292

293

294

295

296

297

298

299

300

301

302

303

304

305

306

307

308

309

310

311

312

#### Limitations

314

315

316

317

318

319

320

321

322

323

324

325

326

327

328

329

This study has several limitations that should be considered. First, we did not evaluate additional senescence markers beyond TP21 and TP53, such as β-galactosidase activity or indicators of cytoskeletal remodeling, which could more comprehensively confirm a senescence-associated hypertrophic phenotype. Second, the Gamma Knife system produces a high-dose hotspot at the central target, while peripheral regions receive only about 50% of the prescribed isodose. This intrinsic spatial dose variation leads to dose heterogeneity within the irradiated cultures and may have influenced the observed variability in cellular responses. Future work utilizing irradiation methods that allow for more homogeneous dose distributions or applying precise dose mapping will be valuable for verification and refinement of these results. Third, our results are derived exclusively from in vitro studies using Hanwoo muscle-derived satellite cells. Verification in vivo is necessary to determine if analogous morphological and molecular responses are observed in the complex muscle tissue environment under physiological conditions. Fourth, this study used cells from a single Hanwoo donor because of the limited availability of primary muscle tissue samples from commercial abattoirs in Korea. Although this constraint reduces biological generalizability, the Hanwoo breed is maintained under a nationally coordinated genetic improvement program that ensures relatively uniform genetic backgrounds across individuals. Future studies will include multiple donors to confirm the reproducibility of these findings.

330331

332

333

334

335

336

337

338

339

340

341

342

343

344

345

346

347

348

## **Conclusions**

Our study demonstrates that gamma irradiation has a dose-dependent impact on Hanwoo muscle satellite cells. Exposure to high doses of 10 Gy and 20 Gy resulted in decreased cell viability, reduced adhesion, and lower proliferation rates. These higher doses also induced abnormal cell enlargement and elevated the expression levels of TP21 and TP53, which are indicative of cellular senescence. The mRNA expression of myogenic markers, including MYF5, MYOD1, and MYOG, was significantly downregulated at these high doses. Cells exposed to 2 Gy irradiation showed a slight reduction in proliferation compared to the control group, although the decrease was substantially less pronounced than that observed at 10 Gy and 20 Gy. Cell size remained comparable to that of the control group following 2 Gy irradiation. Interestingly, MYH2 mRNA expression was modestly elevated relative to control, suggesting a possible activation of protective or differentiation-related pathways under low-dose irradiation conditions. Collectively, these results indicate that low-dose gamma irradiation could be non-detrimental or potentially advantageous under specific conditions. Accurate dose regulation is vital for the successful application of irradiation in cultured meat production, balancing microbial safety with the preservation of satellite cell function. Future research should investigate the effects of lower dosages and confirm the findings in relevant animal models. Additionally, a detailed assessment of radiation distribution will be important to enhance the reliability of cellular response measurements

349	
350	
351	Acknowledgments
352	This work was supported by the research grant of the Chungbuk National University Hospital in 2024. This
353	work was supported by Chungbuk National University BK21 program (2025)
354	
355	



## References

- 1. Nguemgo Kouam P, Bühler H, Hero T, Adamietz IA. The increased adhesion of tumor
- cells to endothelial cells after irradiation can be reduced by FAK-inhibition. Radiation Oncology.
- 359 2019;14:1-11.

- 360 2. Nicolay NH, Sommer E, Lopez R, Wirkner U, Trinh T, Sisombath S, et al. Mesenchymal
- 361 stem cells retain their defining stem cell characteristics after exposure to ionizing radiation.
- 362 International Journal of Radiation Oncology\* Biology\* Physics. 2013;87(5):1171-8.
- 363 3. Yin H, Price F, Rudnicki MA. Satellite cells and the muscle stem cell niche.
- 364 Physiological reviews. 2013;93(1):23-67.
- 365 4. Durante M, Formenti SC. Radiation-induced chromosomal aberrations and
- immunotherapy: micronuclei, cytosolic DNA, and interferon-production pathway. Frontiers in
- 367 oncology. 2018;8:192.
- 368 5. Indiarto R, Irawan AN, Subroto E. Meat irradiation: A comprehensive review of its
- impact on food quality and safety. Foods. 2023;12(9):1845.
- Fertey J, Makert GR, Becker P, Finkensieper J, Ulbert S. Low-Energy Electron
- 371 Irradiation Inactivates Viruses in Serum and Maintains Growth-Promoting Properties in Cell
- 372 Culture. Applied Biosafety. 2025.
- 7. Kim S, Jeong J-O, Lee S, Park J-S, Gwon H-J, Jeong SI, et al. Effective gamma-ray
- 374 sterilization and characterization of conductive polypyrrole biomaterials. Scientific reports.
- 375 2018;8(1):3721.
- 376 8. Filipová A, Diaz-Garcia D, Bezrouk A, Čížková D, Havelek R, Vávrová J, et al. Ionizing
- radiation increases primary cilia incidence and induces multiciliation in C2C12 myoblasts. Cell
- 378 Biology International. 2015;39(8):943-53.
- 9. Panzetta V, Pugliese M, Musella I, De Menna M, Netti P, Fusco S. A biophysical
- analysis to assess X-ray sensitivity of healthy and tumour cells. Radiation protection dosimetry.
- 381 2019;183(1-2):116-20.
- 382 10. Sangsuwan T, Haghdoost S. The nucleotide pool, a target for low-dose γ-ray-induced
- oxidative stress. Radiation Research. 2008;170(6):776-83.
- Park S, Park G, Oh S, Park Y, Kim Y, Kim J, et al. Investigating proliferation and
- differentiation capacities of Hanwoo steer myosatellite cells at different passages for developing
- 386 cell-cultured meat. Scientific Reports. 2023;13(1):15614.
- 387 12. Ding S, Wang F, Liu Y, Li S, Zhou G, Hu P. Characterization and isolation of highly
- purified porcine satellite cells. Cell death discovery. 2017;3(1):1-11.
- 389 13. Filippi-Chiela EC, Oliveira MM, Jurkovski B, Callegari-Jacques SM, Silva VDd, Lenz
- 390 G. Nuclear morphometric analysis (NMA): screening of senescence, apoptosis and nuclear
- irregularities. 2012.
- 392 14. Ross NE, Pritchard CJ, Rubin DM, Duse AG. Automated image processing method for
- 393 the diagnosis and classification of malaria on thin blood smears. Medical and Biological
- 394 Engineering and Computing. 2006;44:427-36.
- 395 15. Pincus Z, Theriot J. Comparison of quantitative methods for cell-shape analysis. Journal
- 396 of microscopy. 2007;227(2):140-56.
- 397 16. Livak KJ, Schmittgen TD. Analysis of relative gene expression data using real-time
- 398 quantitative PCR and the  $2-\Delta\Delta$ CT method. methods. 2001;25(4):402-8.
- 399 17. La Verde G, Artiola V, Panzetta V, Pugliese M, Netti PA, Fusco S. Cytoskeleton
- 400 response to ionizing radiation: A brief review on adhesion and migration effects. Biomedicines.
- 401 2021;9(9):1102.

- 402 18. Asaithamby A, Chen DJ. Cellular responses to DNA double-strand breaks after low-dose
- $\gamma$ -irradiation. Nucleic acids research. 2009;37(12):3912-23.
- 404 19. Cordes N, Blaese M, Meineke V, Beuningen DV. Ionizing radiation induces up-
- 405 regulation of functional  $\beta$  1-integrin in human lung tumour cell lines in vitro. International
- 406 journal of radiation biology. 2002;78(5):347-57.
- 407 20. Lee SH, Cheng H, Yuan Y, Wu S. Regulation of ionizing radiation-induced adhesion of
- breast cancer cells to fibronectin by alpha5beta1 integrin. Radiation research. 2014;181(6):650-8.
- 409 21. Blockhuys S, Van Rompaye B, De Rycke R, Lambein K, Claes K, Bracke M, et al.
- 410 Radiation-induced myosin IIA expression stimulates collagen type I matrix reorganization.
- 411 Radiotherapy and Oncology. 2013;108(1):162-7.
- 412 22. Park B, Choi T, Kim S, Oh S. National genetic evaluation (system) of Hanwoo (Korean
- 413 native cattle). Asian-Australasian journal of animal sciences. 2013;26(2):151.
- Seo D, Lee DH, Jin S, Won JI, Lim D, Park M, et al. Long-term artificial selection of
- 415 Hanwoo (Korean) cattle left genetic signatures for the breeding traits and has altered the genomic
- 416 structure. Scientific reports. 2022;12(1):6438.
- 24. Du Y, Zhang J, Zheng Q, Li M, Liu Y, Zhang B, et al. Heavy ion and X-ray irradiation
- alter the cytoskeleton and cytomechanics of cortical neurons. Neural regeneration research.
- 419 2014;9(11):1129-37.
- 420 25. Pramojanee SN, Pratchayasakul W, Chattipakorn N, Chattipakorn SC. Low-dose dental
- 421 irradiation decreases oxidative stress in osteoblastic MC3T3-E1 cells without any changes in cell
- viability, cellular proliferation and cellular apoptosis. Archives of Oral Biology. 2012;57(3):252-
- 423 6.

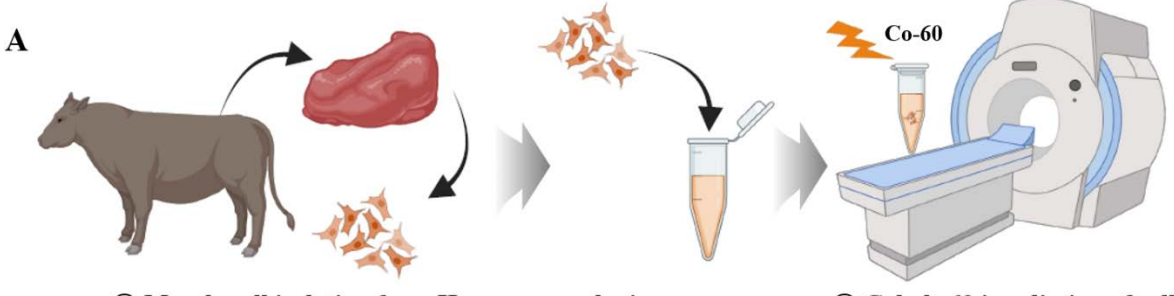
- 424 26. Vaiserman A, Cuttler JM, Socol Y. Low-dose ionizing radiation as a hormetin:
- experimental observations and therapeutic perspective for age-related disorders. Biogerontology.
- 426 2021;22(2):145-64.

Table Table

# Table 1. Sequences of primers used in the RT-qPCR

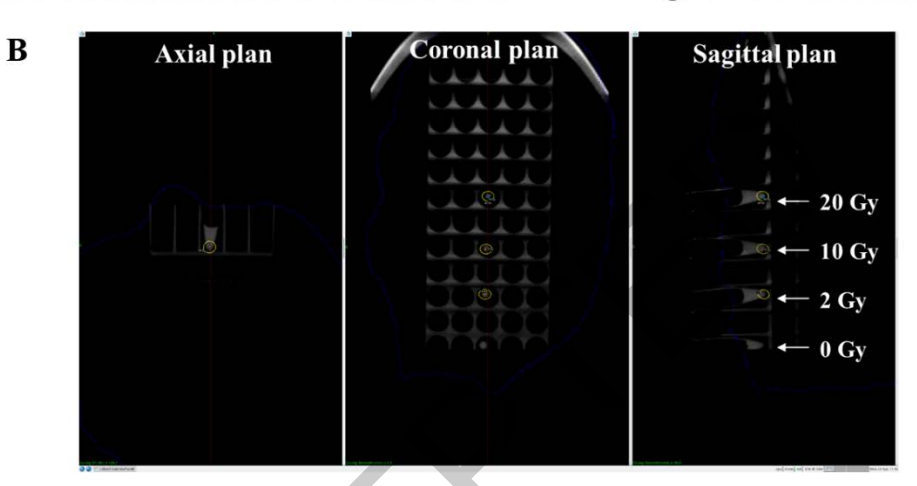
Primer	Description	Accession	Sequence $(5' \rightarrow 3')$	Product size (bp)
MYF5	Myogenic factor 5	NM_174116 -	F: ATTACCAGAGACACCGACCA	184
			R: CAGGAGCCGTCGTAGAAGTA	
MYOD1	Myogenic differentiation 1 NM_001040478	NIM 001040479	F: AACAGCGGACGACTTCTATG	211
		NWI_001040478	R: GTTAGTCGTCTTGCGTTTGC	
TP21	Cyclin-dependent kinase inhibitor 1A (p21)	NM 001098958 -	F: TGCCCTTTCCCCTTAGTATC	241
		NWI_001098938	R: CTGGAAAAATCTGCTCCTCA	
TP53	Tumor protein p53 N	ND 4 174201	F: ATGAGATGTTCCGAGAGCTG	155
		NM_174201 -	R: TCCCTCTCTCTTGAGCATTG	
MYOG	Manager NIM (	NIM 001111225	F: ACAAACCATGCACATCTCCT	215
	Myogenin	Myogenin NM_001111325	R: AGCACAGAGACCTTGGTCAG	
МҮН2	Myosin heavy chain 2 NM_001166227 -	NIM 001166227	F: CCAGTGGAGGACCAAGTATG	227
		R: TTCCTTTGCTTTTTGTCCAG	237	
GAPDH	Glyceraldehyde-3- phosphate dehydrogenase NM_001034034	NIM 001024024	F: ACTCCCAACGTGTCTGTTGT	185
		R: CCAGCATCGAAGGTAGAAGA	163	

Figures Figures



1 Muscle cell isolation from Hanwoo muscle tissue

2 Cobalt-60 irradiation of cells



434435

436

Figure 1. (A) Schematic illustration of Cobalt-60 gamma irradiation applied to primary muscle cells isolated from Hanwoo muscle tissue. (B) Representative axial, coronal, and sagittal plane images showing the targeted irradiation field using the Gamma Knife system.

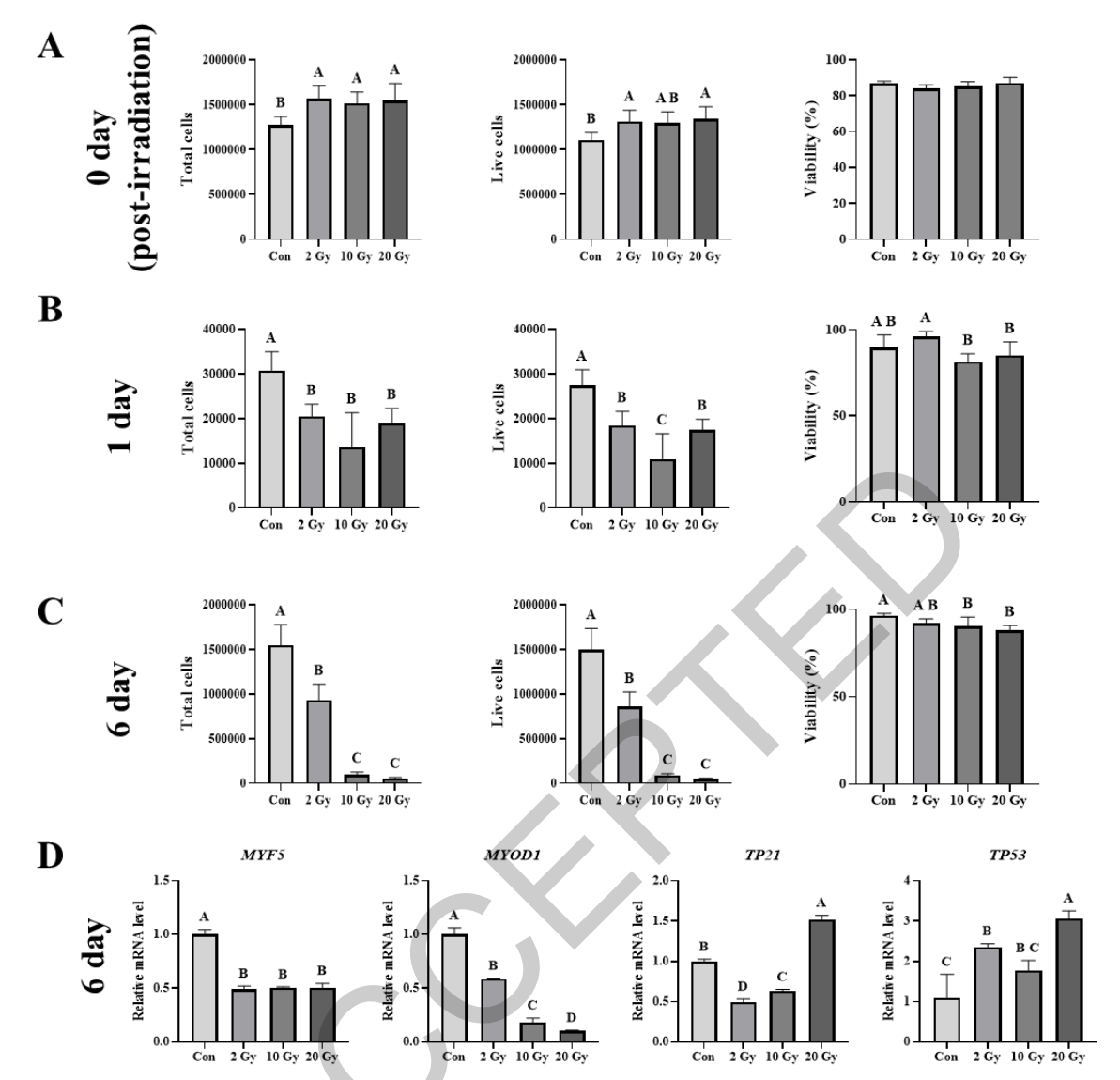


**Figure 2.** (A) Total cell number, live cell number, and viability of Hanwoo muscle-derived cells irradiated with different doses (Con, 2, 10, and 20 Gy) under suspension conditions. (B) Total cell number, live cell number, and viability of irradiated Hanwoo muscle-derived cells after 1 day of culture. (C) Total cell number, live cell number, viability of irradiated Hanwoo muscle-derived cells after 6 day of culture. (D) Relative mRNA expression levels of MYF5, MYOD1, TP21, and TP53 in Hanwoo muscle-derived cells after 6 days of culture under each irradiation dose (Con, 2, 10, and 20 Gy). All mRNA expression levels were normalized to the housekeeping gene GAPDH. Different letters indicate statistically significant differences (p < 0.05, one-way ANOVA followed by Tukey's post hoc test).

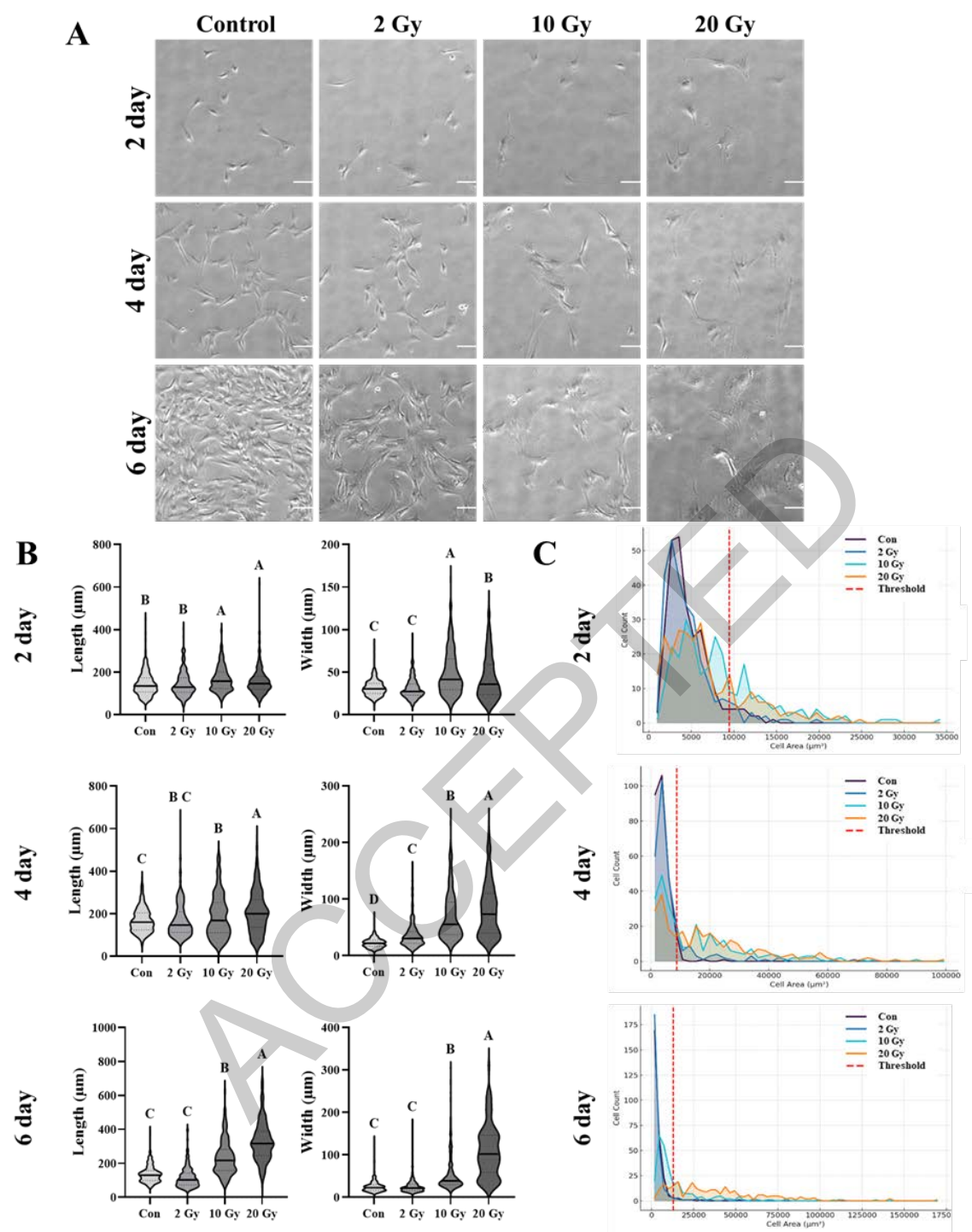


Figure 3. (A) Representative phase-contrast images of Hanwoo muscle-derived cells at 2, 4, and 6 days of culture following gamma irradiation at different doses (Con, 2, 10, and 20 Gy). Magnification:  $40\times$ , Scale bars =  $100~\mu m$ . (B) Quantitative analysis of cell morphology showing cell length ( $\mu m$ ) and width ( $\mu m$ ) at 2, 4, and 6 days post-irradiation in each treatment group. (C) Distribution histograms of calculated cell area (length  $\times$  width) at 2, 4, and 6 days of culture under each irradiation condition. Threshold values were defined as the mean + 2 standard deviations (2SD) of the control (Con) group at each time point. Different letters indicate statistically significant differences (p < 0.05, one-way ANOVA followed by Tukey's post hoc test).

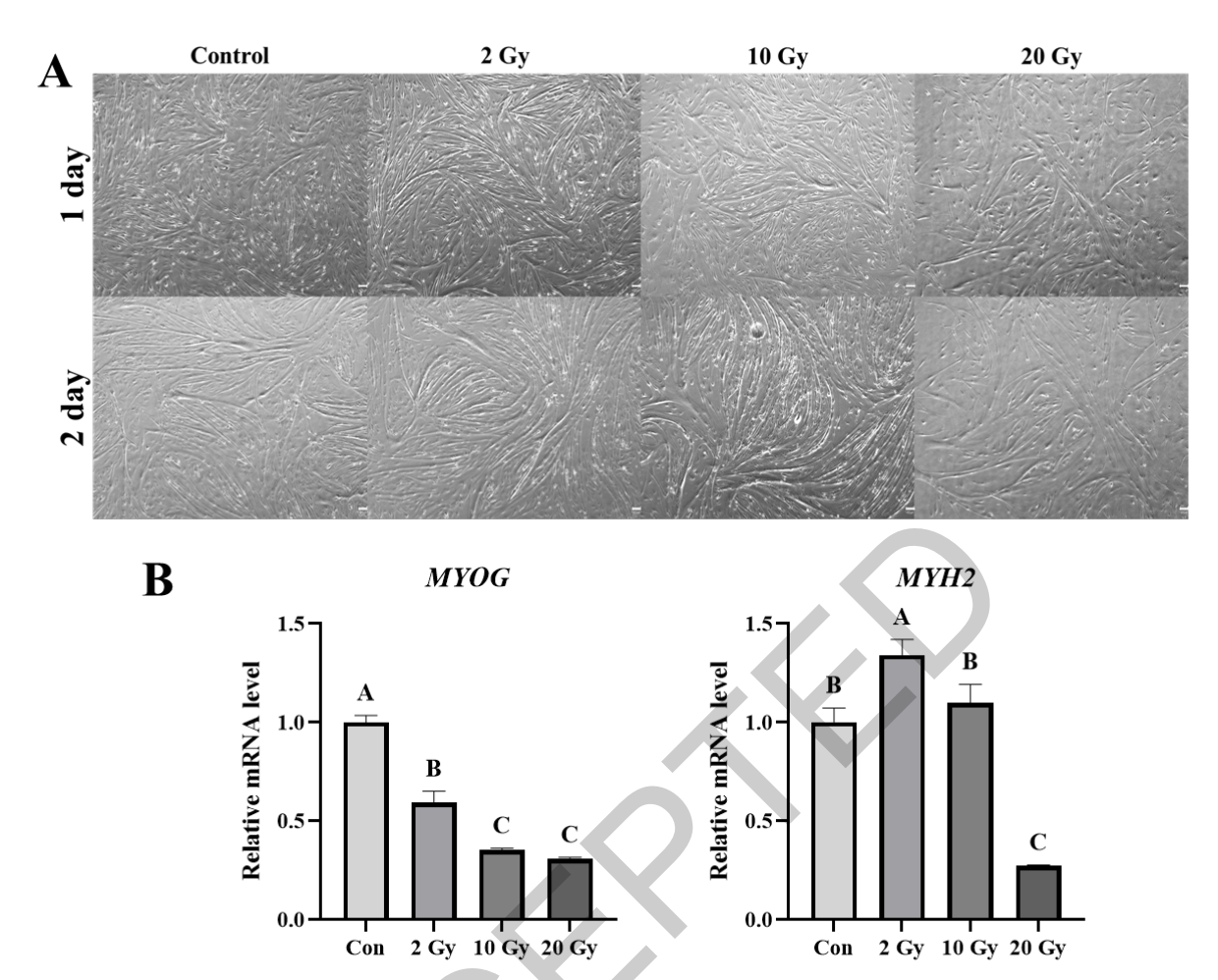


Figure 4. (A) Representative phase-contrast images of Hanwoo muscle-derived cells cultured under differentiation conditions for 1 and 2 days following gamma irradiation at different doses (Con, 2, 10, and 20 Gy). Magnification:  $40\times$ , Scale bars =  $100 \, \mu m$ . (B) Relative mRNA expression levels of *MYOG* and *MYH2* in irradiated Hanwoo muscle-derived cells after 2 days of differentiation culture. All mRNA expression levels were normalized to the housekeeping gene *GAPDH*. Different letters indicate statistically significant differences (p < 0.05, one-way ANOVA followed by Tukey's post hoc test).